Evidence for a sharp interface between partially miscible polymers from a study by neutron specular reflection

M. L. Fernandez and J. S. Higgins
Imperial College of Science and Technology, Chemical Engineering Department, Prince Consort Road, London SW7 2BY, UK

and J. Penfold and C. Shackleton
Neutron Science Division, Rutherford Appleton Laboratory, Chilton, Didcot, Oxon OX11 0QX, UK

and D. J. Walsh
Central Research and Development, E.I. DuPont de Nemours, Wilmington, Delaware 19898, USA
(Received 14 August 1989; revised 20 October 1989; accepted 15 December 1989)

The use of the specular reflection of neutrons to study the nature of the interface between the partially miscible polymers poly(methyl methacrylate) (PMMA) and solution-chlorinated polyethylene (SCPE) is reported. The upper, PMMA, layer has an increasing density gradient towards the surface, and after short annealing times the density of the PMMA increases. Further annealing causes a swelling of the SCPE by the PMMA and diffusion occurs predominantly on the SCPE side of the interface. The PMMA/SCPE interface moves toward the PMMA side but the width of the interface remains approximately constant.

(Keywords: neutron specular reflection; polymer interfaces; polymer blends; interdiffusion)

INTRODUCTION

The structure and composition profile of the interface between two polymeric species is of much current interest, while the thermodynamic theories[1–3] describing the formation of polymer interfaces are controversial. Technologically, the degree of interfacial mixing between components in a binary mixture is important to problems in adhesion, mixing and welding[4,5]. Various experimental techniques have been applied to the investigation of the composition profile of the interface and these include infra-red spectroscopy[6], X-ray microanalysis[7], forward recoil spectrometry (FReS)[8] and Rutherford back-scattering (RBS)[9]. Although these techniques have proved very successful in the study of long-range effects, their resolution (of the order of tens of nanometres) is not sufficient to investigate the short-range detail of the polymer–polymer interface. The specular reflection of neutrons has, however, recently been shown to be a technique capable of probing such interfaces on a dimension scale smaller than is possible by these other techniques, and it has recently been applied by these authors to study the nature of the interface between the immiscible polymer pair polystyrene/poly(methyl methacrylate)[10].

We report here some preliminary results from the application of the specular reflection of neutrons to the study of the nature of the interface between the partially miscible pair of polymers, solution-chlorinated polyethylene (SCPE) with poly(methyl methacrylate) (PMMA), subjected to annealing treatment.

0032-3861/90/112146-06

EXPERIMENTAL

The polymers used in this work were hydrogenous solution-chlorinated polyethylene (h-SCPE) with 63% by weight chlorine content, and deuterated poly(methyl methacrylate) (d-PMMA). The choice of the deuterated PMMA is in order to provide a good 'contrast' at the interface for the neutron reflection study. The characteristics of these polymers are summarized in *Table 1*. The chlorination procedure for the preparation of the SCPE was described by Chai *et al.*[11]. The relatively low molecular weight of the d-PMMA sample was achieved by irradiating fully deuterated PMMA of very high molecular weight with γ radiation. The dose was approximately 36 Mrad[12].

A similar d-PMMA/h-SCPE blend has been previously studied by small-angle neutron scattering, but in this case the h-SCPE had a chlorine content 66% by weight. The blend previously studied shows a miscibility gap with a lower critical solution temperature (*LCST*) at 124°C for a 25% h-SCPE, and for a 50/50 composition the spinodal temperature is 146°C[13]. Since the chlorine content of the h-SCPE strongly influences the position of the phase boundary[14], the miscibility gap for our system will be shifted towards lower temperatures. By scaling the results for the d-PMMA/h-SCPE system to the chlorine content of our h-SCPE[15] and the molecular weight of the d-PMMA[14], we find that the blend h-SCPE/d-PMMA will present a miscibility gap as shown in *Figure 1*. The reason for calculating the position of the phase boundary by scaling procedures rather than measuring it experi-

Table 1 Characteristics of the polymers used in this work

Polymer	$M_w \times 10^{-5}$ ($g\,mol^{-1}$)	$M_n \times 10^{-5}$ ($g\,mol^{-1}$)	*PD*	T_g (°C)	Cl (%)
h-SCPE	2.07	9.17	2.26	116.3	63
d-PMMA	0.37	0.23	1.59	106.5	–

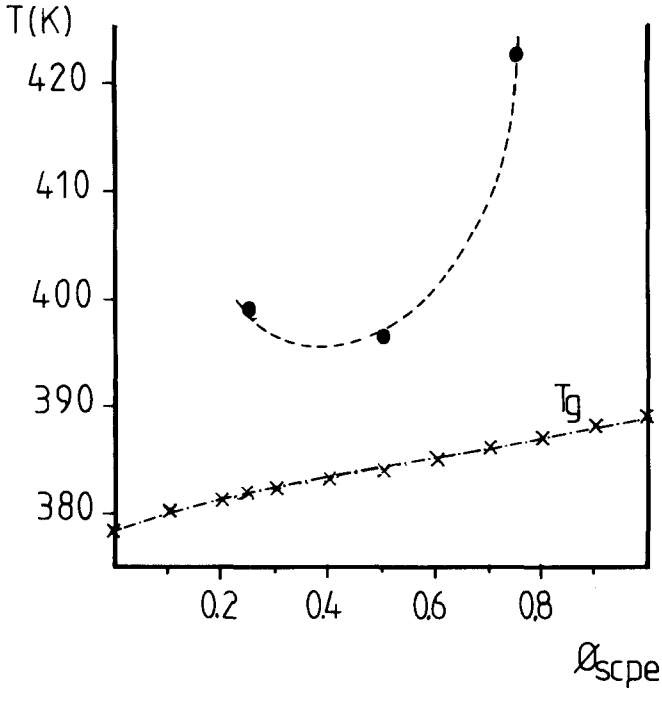

Figure 1 Scaled phase diagram for our system and T_g values predicted by the Fox equation. The full circles represent the points that have been scaled and the broken curve has been drawn through them

mentally is because these experiments cannot be carried out with laboratory techniques. As reported[13], the phase separation takes place over a dimension scale small compared with the wavelength of light.

The sample prepared for the neutron reflection experiment consisted of a film of d-PMMA (approximately 1000 Å) on top of a thick layer (approximately 2800 Å) of h-SCPE, both films being supported on an optical flat. The bottom film was prepared by spinning (at 1000 r.p.m.) a 5% w/v solution of h-SCPE in cyclohexanone directly onto the optical flat, and it was stored under vacuum at 90°C for 22 h before being coated with the d-PMMA. The top layer was prepared by spinning (at 1000 r.p.m.) a 2.5% solution of d-PMMA in cyclohexanone on a glass slide; this film was then floated off the slide on a water bath and transferred to the coated optical flat. The bilayer was then stored under vacuum at 40°C for 22 days prior to the experiments.

The manufactured bilayers were measured by neutron specular reflection before and after a series of annealing treatments at 120°C (see *Table 2*).

The annealing temperature was chosen so that it was above the glass transition temperatures of both polymers where the polymer chains were mobile, but below the critical temperature in order to allow interfacial mixing to occur (see *Figure 1*).

The neutron reflection measurements were carried out at the ISIS pulsed neutron source, Rutherford Appleton Laboratory, on the CRISP reflectometer[16]. A polychromatic neutron beam (wavelength 0.5–6.5 Å) is incident on the polymer film at a fixed glancing angle of 0.5°. The reflection from the film is measured at the specular angle by a single well collimated detector. The wavelength dependence of the reflected neutron intensity is obtained by a time-of-flight analysis.

The reflected intensity is converted to reflectivity by removal of the incident spectral shape (using an incident beam monitor), corrected for the detector efficiency and normalized to unity at total reflection. The calculation of the specular reflectivity profiles can be done exactly for any model profile using the optical matrix method[17]. In this paper we use the optical matrix method and optimize fits to the data using a non-linear least-squares routine[18].

RESULTS

Figure 2 shows a typical reflectivity profile for a d-PMMA/h-SCPE bilayer film. The interference pattern arises from waves reflected at each interface. The dominant lower-frequency fringes result from the thinner top layer of d-PMMA, whereas the higher-frequency pattern superimposed on it arises from the thicker lower layer of h-SCPE.

Figure 3 shows the reflectivity profiles for the d-PMMA/h-SCPE bilayer following the annealing sequences in *Table 2*. There was no measurable change in the profile following the initial annealing (A) and therefore it has not been included in *Figure 3* or in the subsequent discussion. Without detailed numerical analysis, a number of important observations can be made. The position of the total reflection and the

Table 2 Annealing times for the bilayer d-PMMA/h-SCPE

Annealing time (min)	Annealing code	Cumulative annealing time (min)
5	A	5
+15	B	20
+15	C	35
+15	D	50
+30	E	80
+15+60	F	155
+120	G	275

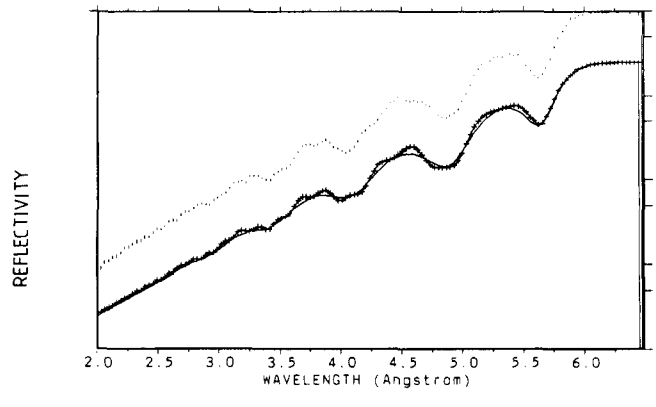

Figure 2 Reflectivity profile for the sample as made. The error bars represent the experimental data. The single full curve corresponds to the pattern arising from the d-PMMA and the full curve marked with crosses shows the contribution of both the d-PMMA and the h-SCPE. The profiles have been shifted for clarity

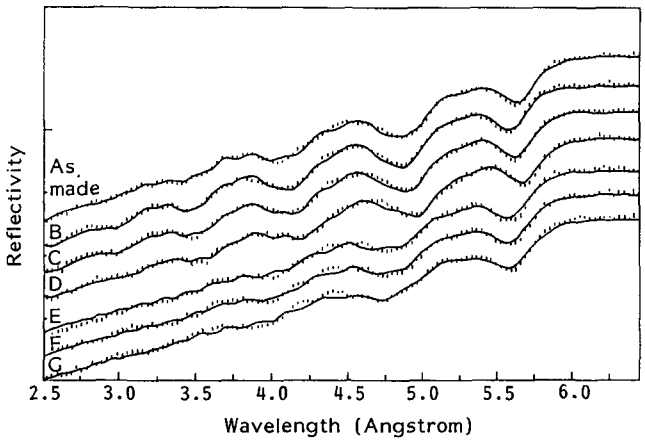

Figure 3 Reflectivity profile for the sample as made and for the six annealing processes; the patterns have been shifted for clarity. The angle of incidence of the neutrons was $\theta = 0.5°$ in all cases

spacing of the lower-frequency fringes are determined predominantly by the density and thickness of the d-PMMA layer, and the rate at which those fringes damp is determined by the width and nature of the d-PMMA/h-SCPE interface. The density and thickness of the lower h-SCPE layer determine the contribution due to the high-frequency fringes; but the predominant features of the reflectivity pattern are much less sensitive to these parameters and to the density of the substrate.

In order to obtain an initial quantitative assessment of the annealing process, and to indicate clearly the major processes in operation, the initial model fitting has been made using a single bilayer with a diffuse Gaussian interface at the d-PMMA/h-SCPE interface. In view of the lack of sensitivity of the main features of the reflectivity profile to the thickness and density of the lower h-SCPE layer and the density of the substrate, these parameters have been held constant in the refinement procedure (see *Table 3* for the fixed values). The fitted parameters (thickness and density of the d-PMMA layer, and the width of the interface) are summarized in *Table 3* and illustrated in *Figure 4*.

The following effects have been observed on the thickness and on the density of the d-PMMA film. During annealings B, C and D the thickness of the top layer increases. After annealing B the density of the d-PMMA increases and then remains approximately constant during annealings C and D. This suggests that during the first three annealing processes the d-PMMA layer is stabilizing and that the chains are allowed to more and arrangement themselves until they reach equilibrium.

After annealings E, F and G the thickness of the top layer decreases and its scattering length density remains constant. The root-mean-square roughness of the interface initially increases from 70 to 90 Å and then remains constant, as shown by σ_{12} in *Table 3*.

It is clear that, although the single two-layer model reproduces well and explains the main features of the reflectivity profiles, some discrepancies do exist. In particular, the high-frequency fringes are not perfectly matched; this can be improved by further refinement of the model, but as it does not affect the subsequent conclusions, it has been pursued no further at this stage.

The other main discrepancy is that beyond the region of total reflection the model calculation lies at consistently lower reflectivities than the data. This effect has also recently been observed on some single films of d-PMMA and was attributed to an increasing density gradient at the surface of the d-PMMA. We have for this system eliminated other possible contributions and conclude that the upper d-PMMA layer also has an increasing density gradient at the surface. In practise, we have modelled the density gradient by introducing an additional layer at the surface of the d-PMMA; and in the model the thickness and density of each layer in addition to the width of the d-PMMA/h-SCPE interface has been refined. The fitted parameters are summarized in *Table 4*, and an example of the improved quality of fit over that shown in *Figure 4* is shown in *Figure 5*. All the profiles have been fitted with resolution $d_{th} = 3.5\%$ and $N_b(\text{glass}) = 0.355 \times 10^{-5}$ Å^{-2}, where N_b stands for scattering length density. The thickness of the h-SCPE layer was fitted as 2752 Å for annealings B, C and D and from then onwards it increased up to a value $d = 2910$ Å for annealing G. Similarly, the scattering length density was taken approximately constant until annealing D, $N_b = 0.19 \times 10^{-5}$ Å^{-2} (which agrees well with calculated values and with previous measurements) and then increased up to $N_b = 0.24 \times 10^{-5}$ Å^{-2} for annealing G.

The main observations for the model fits are similar to those for the simpler model, but there is now some additional information. The density gradient in the d-PMMA does not disappear with annealing. It is also evident that the thickness and density of the h-SCPE layer increase with annealing; however, the parameters associated with that layer are not too precise.

DISCUSSION

One of the main features shown by the data is the presence of a density gradient in the d-PMMA layer. The

Table 3 Parameters used in the two-layer fits of the reflectivity profiles, where N_b and d are the scattering length density and thickness of the d-PMMA and σ is the root-mean-square roughness of the d-PMMA/h-SCPE interface. All the profiles have been fitted with the following constant parameters: resolution $d_{th} = 3.5\%$, $N_b(\text{h-SCPE}) = 0.17 \times 10^{-5}$ Å^{-2}, $d(\text{h-SCPE}) = 2660$ Å and $N_b(\text{glass}) = 0.355 \times 10^{-5}$ Å^{-2}

Annealing code	d (Å)	$N_b \times 10^5$ (Å^{-2})	σ_{12} (Å)
As made	972	0.56	70
B	960	0.675	70
C	1003	0.687	55
D	1020	0.698	70
E	960	0.677	90
F	943	0.67	90
G	922	0.66	90

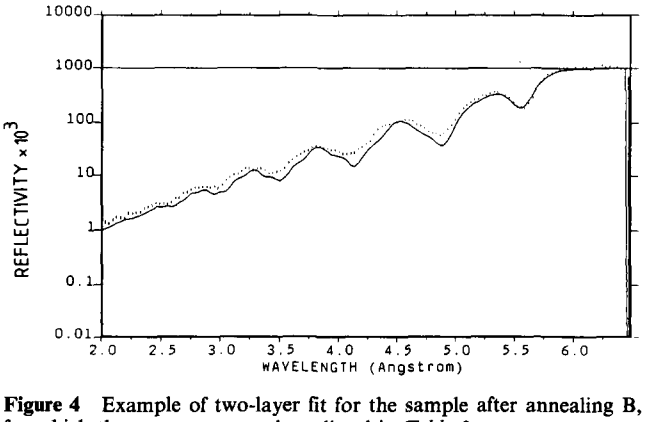

Figure 4 Example of two-layer fit for the sample after annealing B, for which the parameters used are listed in *Table 3*

Table 4 Parameters used in the three-layer fits of the reflectivity profiles. N_{b1} and d_1 represent the scattering length density and thickness of the 'top d-PMMA layer' and N_{b2} and d_2 are the corresponding values for the 'bottom d-PMMA layer'. σ_{12} and σ_{23} represent the root-mean-square roughness between the two d-PMMA 'layers' and between the d-PMMA and the h-SCPE, respectively

Annealing code	d_1 (Å)	$N_{b1} \times 10^5$ (Å^{-2})	σ_{12} (Å)	d_2 (Å)	$N_{b2} \times 10^5$ (Å^{-2})	σ_{23} (Å)
As made	148	0.71	30	812	0.66	70
B	132	0.74	47	858	0.68	56
C	135	0.73	52	859	0.67	63
D	142	0.71	58	868	0.66	70
E	200	0.70	51	738	0.66	90
F	195	0.70	58	737	0.67	90
G	178	0.693	51	719	0.66	90

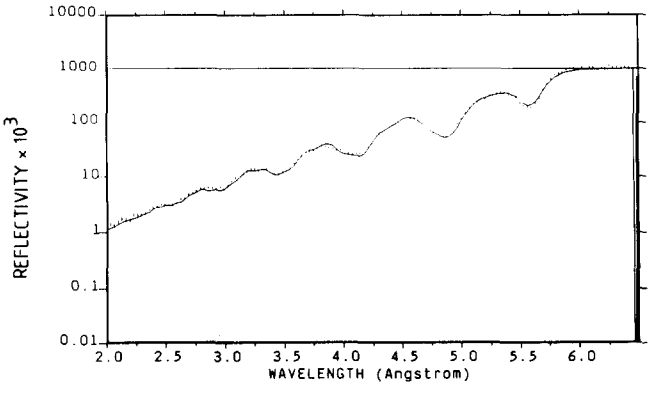

Figure 5 Example of three-layer fit for the same as made, for which the parameters shown in *Table 4* have been used

magnitude of the densities is not consistent with a mixed d-PMMA/h-SCPE intermediate layer at the interface, and correspond to a real density gradient in the d-PMMA. Furthermore, the d-PMMA density increases during the initial annealing as opposed to the decrease that would be expected from true intermixing. This densification with annealing has also been observed in similar experiments for the d-PMMA/h-PS system[10].

As anticipated, the width of the polymer/polymer interface for this system (reflected in the value of σ_{23} in *Table 4*) is not as sharp as that of an immiscible system[10]. After annealing B, the quality of the sample improves; the d-PMMA chains are allowed to move and arrange themselves as flat as possible so that the interfacial roughness decreases. During annealings C and D the sample is still equilibrating; the thickness and scattering length density of the overall d-PMMA layer increase but no significant polymer–polymer diffusion takes place.

After annealing E the first hints of polymer diffusion are observed. These are characterized by increases in the scattering length density of the bottom layer and in the width of the interfaces, and suggest that there is some mixing between the h-SCPE and the d-PMMA.

The question might arise whether the changes observed in the scattering length density of the SCPE are due to diffusion or to a loss of water that might have penetrated the film during the floating and evaporated on annealing at 120°C. However, three factors indicate that this is not the case. First, the value $N_b = 0.19 \times 10^{-5}$ Å^{-2} for SCPE agrees well with calculated values and with previous measurements. Secondly, if the change is scattering length density from $N_b = 0.19 \times 10^{-5}$ to 0.24×10^{-5} Å^{-2} was due to water loss, the original SCPE film would contain 17% water, which is a rather large quantity. Finally, if such an amount of water had evaporated when annealing at 120°C, this would have resulted in a thinning of the SCPE film. However, the opposite effect has been observed.

The interface has been modelled as a Gaussian, and this implies that there is some mixing on both sides of the interface. However, if the process that we are describing was 'real' diffusion, one should observe a corresponding decrease in the scattering length density of the d-PMMA layer. The fact that we do not see this change suggests that the diffusion process is occurring in the h-SCPE side of the interface to a greater extent than in the d-PMMA side.

It is, however, clear from our data analysis that from annealing E onwards the thickness of the overall d-PMMA layer decreases and that of the h-SCPE increases, i.e. the interface moves towards the original d-PMMA layer.

These results are in agreement with the recent theory of Brochard and deGennes[19,20] for the diffusion of two species with different diffusion rates. In such a system and for diffusion times smaller than the reptation time, the interface would be a classical error function shape on the side of the slow-moving species with a discontinuity on the other side, as the fast-moving component originally swells the slow component. The interface would move towards the side of the fast-moving component but retain its sharpness. Finally, for diffusion times longer than the reptation time, the step in concentration disappears and the interface broadens (see *Figure 6*).

In this study, since the molecular weight of the d-PMMA is much smaller than that of the h-SCPE and the T_g of the d-PMMA is 10°C lower than that of the h-SCPE, the d-PMMA should move much faster than the h-SCPE. The Brochard and deGennes theory is consistent, at least qualitatively, with our observations: with annealing, the interface moves towards the side of the more mobile component, i.e. d-PMMA, but the width of the interface remains approximately unchanged. Also, mixing is observed to a greater extent on the side of the slow-moving species, i.e. the h-SCPE. According to the above theory, this would mean that rather than true polymer–polymer interdiffusion there is a swelling of the long and slow-moving h-SCPE macromolecules by the short and much faster d-PMMA chains.

According to this theory, the concentration profile in the sample must then show the shape depicted in *Figure 7*: a sharp step on the d-PMMA side and a long tail on the h-SCPE side. The κ range of the data measured here is not sufficient to distinguish between different forms of the interface, and, as a consequence, it is not sensible to discuss in detail the shape of the polymer/polymer interface. It is, however, clear that the diffusion process across the interface is rather asymmetrical in that the diffusion on the side of the h-SCPE has taken place to a greater extent than on the d-PMMA side.

In addition, we have been able to show some quantitative agreement between the Brochard and deGennes theory and our experimental data. The error bars in the annealing times will be quite large because, due to the mass and the thermal conductivity of the glass of which the substrate is made, the jump in temperature is not immediate. The bilayer was supported on an optical flat whose total volume was 20 cm^3 of glass and it was

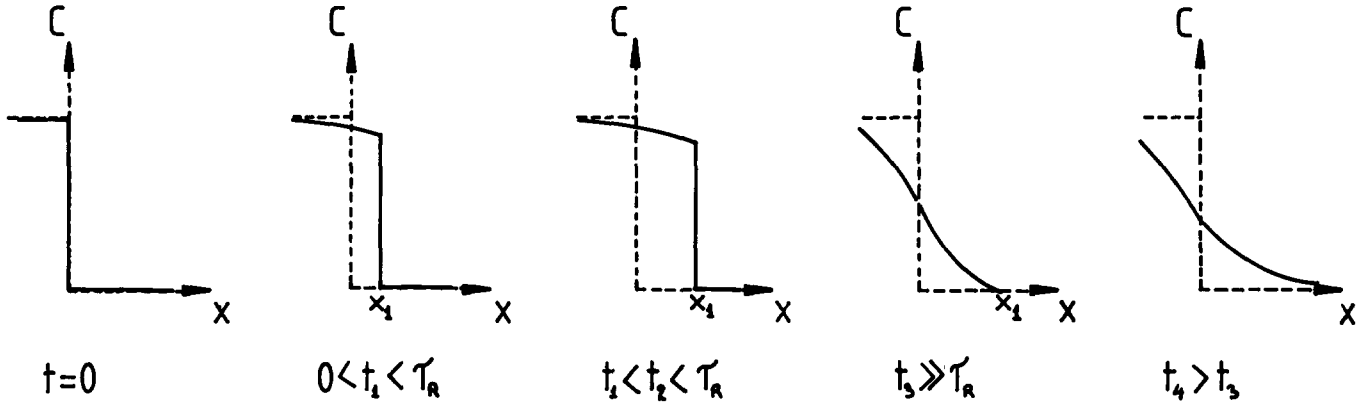

Figure 6 Schematic representation of Brochard and deGennes' prediction for the evolution of the interface between a solvent and a polymer with diffusion time. The original situation corresponds to a perfectly flat interface between pure polymer on the left, and pure solvent on the right. For diffusion periods smaller than the reptation time, the interface presents a sharp step on the side of the solvent and an error function form shape on the side of the polymer. The interface moves towards the solvent side but retains its sharpness. For diffusion periods longer than the reptation time, the interface presents a well defined front whose shift towards the solvent side scales as x_1. In this case, however, the shape of the interface does not present a sharp discontinuity on one side but a power-law increase. For longer diffusing periods, the profile spreads

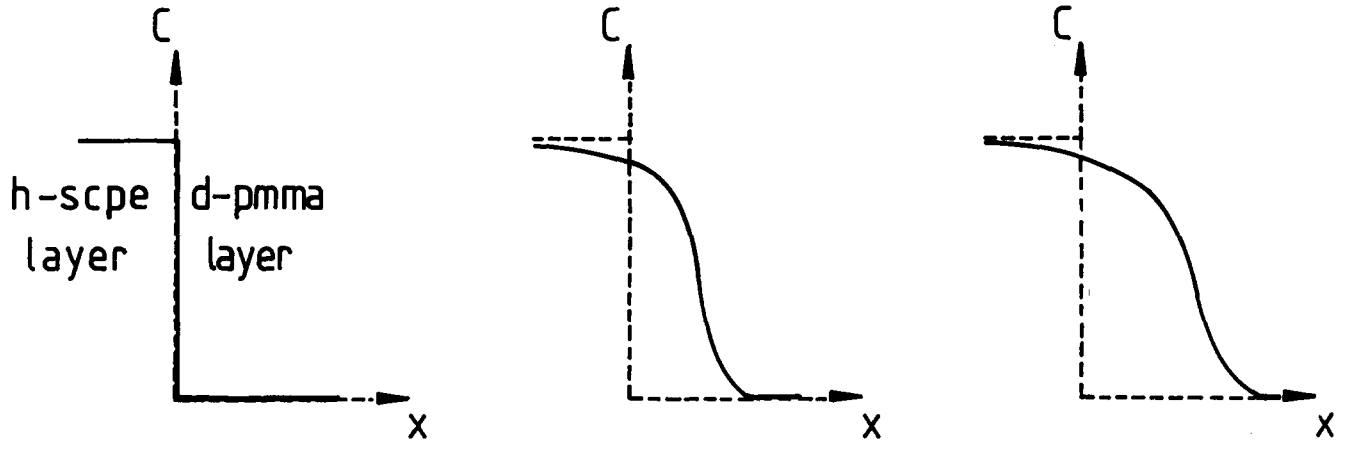

Figure 7 Schematic representation of the Brochard and deGennes theory for our sample, in which we have assumed a Gaussian interface between the two polymers

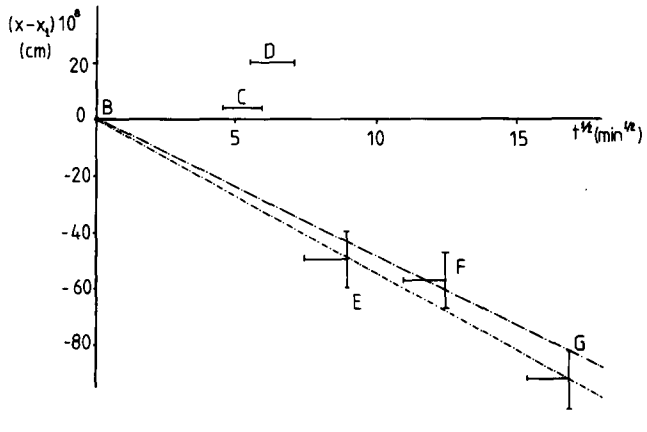

Figure 8 Difference between the thickness of the overall d-PMMA sample for each annealing process and that after annealing B, *versus* the square root of time

annealed in a conventional oven. Since a piece of glass of such a size takes some time in heating and cooling, the effective annealing times will be shorter than those reported here and we have then included an uncertainty of 5 min in each of the annealing periods. There will also be some uncertainty in the annealing temperature due to the fact that the sample experiences a gradient in temperature during heating.

Brochard and deGennes give an expression for the distance that the interface should move as a function of time, as follows:

$$x_1 = c(k_B T/\eta_s \xi)^{1/2} t^{1/2} \quad (1)$$

where k_B is the Boltzmann constant, T is temperature, η_s is the viscosity of the more mobile species, ξ is the average mesh size for the least mobile species, c is a constant and t is time. They do not give any value for the constant c in equation (1).

We have calculated $\eta_s = 2.93 \times 10^7\ g\,cm^{-1}\,s^{-1}$ as the viscosity of the d-PMMA at vanishing shear rate[21]. The average mesh size for a semidilute solution is defined as:

$$\xi(\Phi) = a\Phi^{-3/4} \quad (2)$$

where a is the size of the step in a random walk in a periodic lattice and Φ is the fraction of lattice sites occupied by the slow-moving species. The step length a is defined in terms of the mean-square end-to-end distance $\langle r^2 \rangle$ as[21]:

$$\langle r^2 \rangle(\Phi) = Na^2\Phi^{-1/4} \quad (3)$$

where N is the degree of polymerization of the slow

chains. The mean-square end-to-end distance is related to the radius of gyration R_g, by the expression:

$$\langle r^2 \rangle = 6R_g^2 \quad (4)$$

From equations (2), (3) and (4) and considering molecular weight instead of degree of polymerization ($M_w = NM_0$, where M_0 is the molecular weight of the monomer unit):

$$\xi(\Phi) = R_g \Phi^{-5/8} (6M_0/M_w)^{1/2} \quad (5)$$

For h-SCPE there are no values of R_g in the literature, but the relationship between $\langle R_g^2 \rangle_z^{1/2}$ and $M_z^{1/2}$ is 0.44 for poly(ethylene) and for poly(vinyl chloride), if the increased weight due to chlorine content is taken into account[22,23]. For our h-SCPE then, $\xi \sim 15.4 \times 10^{-8}$ cm. So from equation (1) we get the result that:

$$x_1 = c(1.096 \times 10^{-7} \text{ cm s}^{-1/2}) t^{1/2} \quad (6)$$

Formally, equations (1) to (5) are restricted to semidilute solutions in good solvents. These expressions would therefore require some modifications to cover the concentrated regime. However, as the authors point out[19], this simple scaling approach should be of help at least as a starting point.

In *Figure 8* we have plottted the difference between the thickness of the d-PMMA layer for each of the annealing processes and that of annealing B, *versus* the square root of the diffusion time. We have thus considered the sample after annealing B as our 'original' sample. We have included an uncertainty of 5 min and of ± 10 Å for each of the annealings. The slope of such a plot is: slope $= -5.23 \times 10^{-8} \pm 0.375 \times 10^{-8}$ cm s$^{-1/2}$, the sign being negative because the interface moves towards the surface. We have ignored the points corresponding to annealings C and D because, as we said before, we believe that at this point the sample was still equilibrating. The linearity in *Figure 8* is fairly good and if we were to predict a value for the constant in equation (6) this would be 0.477 from our experimental data. One should be cautious when giving numerical values for a system like ours in which so many parameters are approximate; nevertheless, the important conclusion is that the theory proposed by Brochard and deGennes predicts not only the qualitative behaviour of our sample but also the relationship between the position of the interface and the annealing time.

CONCLUSIONS

We have observed diffusion in d-PMMA/h-SCPE pairs with annealing at a temperature above the glass transition temperatures of both polymers.

The d-PMMA shows some interesting properties, which are functions of thin films, not interfacial mixing. The d-PMMA layer shows a density gradient that increases towards the surface. After a short annealing, the density of the overall d-PMMA layer increases. With further annealing the denser top material starts to diffuse into the rest of the d-PMMA.

Further annealings cause the d-PMMA chains to swell the h-SCPE so that diffusion is observed on the h-SCPE side of the interface to a greater extent than on the d-PMMA side. The polymer/polymer interface retains its thickness while moving towards the d-PMMA side.

The theory proposed by Brochard and deGennes for diffusing pairs of very different mobilities predicts qualitatively and quantitatively the phenomena shown by our sample.

ACKNOWLEDGEMENTS

The authors wish to thank Dr R. E. Hill for the preparation of the h-SCPE and the γ 'chopping' of d-PMMA.

REFERENCES

1 Binder, K. *J. Chem. Phys.* 1983, **79**, 6387
2 Kramer, E. J., Green, P. F. and Palmstrom, C. J. *Polymer* 1984, **25**, 393
3 Sillescu, H. *Makromol. Chem. Rapid Commun.* 1987, **8**, 393
4 Meier, D. J. 'Polymer Blend Mixtures', NATO ASI Ser. E, No. 89, 1985
5 Nielsen, L. E. 'Mechanical Properties of Polymers', Marcel Dekker, New York, 1974
6 Klein, J. and Briscoe, B. J. *Proc. R. Soc. Lond.* (*A*) 1979, **365**, 53
7 Goldstein, J. I., Newbury, D. E., Echlin, P. E., Coy, D. C., Fiori, C. and Lifshin, E. 'Scanning Electron Microscopy and X-ray Microanalysis', Plenum, New York, 1981
8 Turos, A. and Meyer, O. *Nucl. Instrum. Meth.* 1984, **232**, 92
9 Chu, W. K., Mayer, J. W. and Nicolet, M. A. 'Backscattering Spectrometry', Academic Press, New York, 1978
10 Fernandez, M. L., Higgins, J. S., Penfold., J. Ward, R. C., Shackleton, C. and Walsh, D. J. *Polymer* 1988, **29**, 1923
11 Walsh, D. J., Higgins, J. S. and Chai, Z. *Polym. Commun.* 1982, **23**, 336
12 Prentice, P. *J. Mater. Sci.* 1985, **20**, 1445
13 Higgins, J. S., Fruitwala, H. A. and Tomlins, P. E. *Br. Polym. J.* in press
14 Chai, Z., Sunkuona, H., Walsh, D. J. and Higgins, J. S. *Polymer* 1983, **24**, 263
15 Hill, R. E. PhD Thesis, Imperial College, London, 1985
16 Penfold, J., Ward, R. C. and Williams, W. G. *J. Phys.* (*E*) *Sci. Instrum.* 1987, **20**, 1411
17 Born, M. and Wolf, E. 'Principles of Optics', 6th Edn, Pergamon Press, Oxford, 1980
18 Penfold, J. *J. Physique* in press
19 Brochard, F. and de Gennes, P. G. *Phys. Chem. Hydrodyn.* 1983, **4**, 313
20 Brochard, F. and de Gennes, P. G. *Europhys. Lett.* 1986, **1**, 221
21 deGennes, P. G. 'Scaling Concepts in Polymer Physics', Cornell University Press, Ithaca, NY, 1979
22 Lieser, G., Fischer, E. W. and Ibel, K. *J. Polym. Sci.* 1975, **13**, 39
23 Hershenroder, P. and Dettenmaier, M., Private communication